DETECTION OF UNDERGROUND ANOMALIES BY STUDYING THEIR DAMPING EFFECTS ON RAYLEIGH WAVES

Ali Nasseri Moghaddam, University of Waterloo, Waterloo, ON
Giovanni Cascante, University of Waterloo, Waterloo, ON
Chris Phillips, Golder Associates Ltd., Missisuga, ON
Jean Hutchinson, Queen's university, Kingston, ON

ABSTRACT
The Finite differences method is used to simulate the Multi-channel Analysis of Surface Waves (MASW) test method. A homogeneous model is constructed, and voids with different dimensions and embedment depths are introduced in it. Vertical and horizontal surface displacement components are recorded in time domain. To locate the void, the recorded signals are analyzed in time and frequency domains. Both analyses are found to be sensitive to the change in embedment depth and size of the anomaly. Relative attenuation of the propagated wave is used to locate the void and estimate its embedment depth (Attenuation Analysis of Rayleigh Waves – AARW- method). The effectiveness of this method for locating a void and estimating its embedment depth is further studied. Different conditions are investigated such as: different material properties and source types. Also the effects of surface topography, and ambient noise on the responses are studied.

RESUMÉ
La méthode finie de différences est employée pour simuler la methode d'analyse multicanale des vagues extérieures (AMVE). Un modèle homogène est construit, et des vides avec différentes dimensions et profondeurs d'embedment sont présentés dans lui. Des composants extérieurs verticaux et horizontaux de déplacement sont enregistrés dans le domaine de temps. Pour localiser le vide, les signaux enregistrés sont analysés dans des domaines de temps et de fréquence. Les deux analyses s'avèrent sensibles au changement de la profondeur d'embedment et de la taille de l'anomalie. L'atténuation relative de la vague propagée est employée pour localiser le vide et pour estimer son profondeur d'embedment (la méthode d'analyse d'atténuation d'ondule Rayleigh - AAOR). L'efficacité de cette méthode pour localiser un vide et estimer son profondeur d'embedment est encore étudiée. Différentes conditions sont étudiées comme les propriétés des materiaux et les types de source. Les effets de la topographie extérieure et le bruit ambiant sur les réponses sont aussi étudiés.

1 Introduction

Various NDT methods have been developed and used in Geotechnical engineering with different degrees of success. In general, geophysical NDT methods can be classified into: potential field methods (i.e. gravity methods), seismic methods (i.e. seismic reflection surveying, seismic refraction surveying), electrical methods (i.e. electrical resistivity) and electromagnetic methods (i.e. ground penetrating radar)(Reynolds 1997). Spectral analysis of surface waves (SASW) is a seismic method that employs Rayleigh waves (R-waves) to estimate the in-situ low strain shear moduli (strains less than 0.001%) of different layers of soils (Nazarian et al. 1984). Recent studies on surface waves showed that it is a promising tool for characterizing the soil as well as detecting the embedded anomalies and mines (Gucunski et. al. 1996, Phillips et. al. 2001, Nasseri-Moghaddam et. al. 2004). A wide variety of geophysical non-destructive methods can be used for detection of anomalies and material characterization; however, their applicability is not universal and therefore complementary measurements with different methods have higher chances of success. Hence there is a crucial need to introduce and put into application a standard, and generally accepted NDT method to characterize soils with vertical or lateral in-homogeneities.

R-waves fulfill many non-destructive testing requirements, although their behaviour in non-homogeneous media is not well understood. R-waves could be generated and recorded easily. They carry a large amount of energy at the surface layers and attenuate with distance less than body waves (Miller and Pursey 1954). Moreover, their penetration depth depends on the wavelength. Hence, the dispersive characteristic -frequency dependent velocity- of the R-waves can be used to estimate the shear moduli of different layers of soil in a vertically non-homogeneous medium. The propagation of R-waves in homogeneous and horizontally layered media has been studied thoroughly in the past century, a detailed review of the studies can be found in Graff (1991). On the other hand, despite of the advances made in studying the behaviour of R-waves in laterally non-homogeneous media (Gucunski et al. (1996), Phillips et al. (2001)) enough theoretical and practical data is not available in this field.

Theoretical solutions (Lamb 1904, Graff 1991) showed that the nature of particle motion due to R-wave is elliptical and retrograde with respect to the direction of propagation. The amplitude of R-waves at surface decays with distance. In a homogeneous medium, this attenuation is due to material damping (Intrinsic damping) and geometrical damping. The geometrical damping is not frequency dependent and for low-strain cases (as in a SASW test) the material damping is also considered

frequency independent. In non-homogeneous media, another type of damping exists which is called apparent attenuation (Santamarina et al. 2001): in the presence of interfaces (i.e. layers, voids) reflection and mode conversion happen, and only part of the wave energy is transmitted. This type of damping is frequency dependent in all media. In general, the total attenuation in a lossy media is due to the material damping, geometrical damping and apparent attenuation.

Several researchers have developed numerical models to study the behaviour of R-waves in the presence of vertical discontinuities. The works of Al-Hunaidi (1993) revealed that the selection of either a plane or an axisymmetric model is justified for the concept, and that there is a good agreement between the field and numerical data. Gucunski and Woods (1992) showed that for regular soil stratification (i.e. shear stiffness of soil increases with depth) source-to-near receiver spacing has a strong effect on the dispersion curve.

Previous results from models with lateral in-homogeneities (Sheu et al. 1988; Gucunski et al. 1996; Ganji et al. 1998; Phillips et al. 2001) show that the presence of an anomaly causes rippled signals. The ripples are more conspicuous between the source and anomaly (in front of the inclusion); because the obstacle reflects back part of the energy of the incident wave. The width of the anomaly affects the pattern of the ripples and its height and embedment depth affect the amplitude of reflections.

Based on the attenuation characteristics of the R-waves, a quantitative method has been developed by the authors (Nasseri-Moghaddam et. al. 2004) for determining the location of a void and estimating its embedment depth, which is called Attenuation Analysis of Rayleigh Waves method (AARW). The objective of this paper is to give a better insight into the capabilities of the AARW method in different conditions. A calibrated finite differences model is used to simulate the propagation of R-waves in a non-homogeneous medium. When R-waves encounter a void, their energy is reflected, transmitted, and converted into body waves. The transmitted waves are highly attenuated. Based on the latter observation, the new procedure is developed to detect anomalies. The AARW method can be used not only to detect a void but also to estimate its embedment depth. The method is systematic and quantitative and is verified with its application to different models. The method works well in the presence of noise. Further, the effects of different types of sources and uneven surfaces on the output of the method are addressed.

2 The SASW and MASW methods

The SASW test method evolved from the steady-state R-wave method (Jones 1962), and was further developed by Nazarian et al. (1984) and other researchers. The SASW method is based on the dispersion of surface-wave in layered media. Dispersion arises because waves of different wavelengths deform different sections of the layered medium. As frequency increases, the penetration of surface waves decrease. Thus, higher frequencies will probe the properties of shallower strata. For practical purposes, the maximum depth of penetration can be considered to be two to three times the wavelength (Stokoe and Nazarian 1985).

To carry out SASW tests in the field, two transducers (i.e. geophone) are deployed in a line at a certain distance from a source. The distance between the source and first receiver determines the largest developed wavelength in the measurements; furthermore, it controls the near field effect. On the other hand, the distance between the transducers determines the smallest obtainable wavelength from the data. The source should produce enough energy in a wide frequency range. A very common source is a steel hammer; though more complicated sources with better control over the frequency range are also available commercially. As an advancement of the SASW method, several transducers have been utilised for collecting data. Capability for effective noise removal, identification of higher modes of Rayleigh waves, and speed of data collection procedure are among the advantages that made the multi-channel analysis of surface waves (MASW) method more attractive in recent years.

The recorded signals are analysed in the time and frequency domains. From the time plots the group velocities and the contaminating effects of body waves can be estimated; also the location of strong reflections and diffractions can be determined. Using spectrum analyzer, the collected data can be transformed into the frequency domain in real time. From the frequency domain records, the power and phase spectrums, coherence functions, power densities, dispersion curves, and attenuation ratios are computed. The two latter parameters have important role in SASW and AARW methods.

The spectral amplitudes of the signals can also be used to calculate the attenuation of surface displacements. The geometrical and material attenuation - for low-strain loading - are frequency independent (Lamb 1904; Hardin et al. 1972; Hall et al. 1964), so their effects can be constant in frequency domain analysis. Thus the only type of attenuation that is frequency dependent is the one produced by the scattering and mode conversion of the wave fronts (Apparent attenuation).

3 Numerical study

Due to the unavailability of a closed form solution for the propagation of R-wave in a non-homogeneous medium, the use of a numerical model for this study is unavoidable. A numerical model is versatile, cheap, and can be run under controlled testing conditions (i.e. geometry, material properties, source type). Moreover, if the model is designed and calibrated properly, reliable results will be obtained, which are not contaminated with unwanted

noise. The final results of a numerical study should be verified by field data. The numerical model is developed for this study is described next.

4 Conceptual model

To simulate wave propagation in a non-homogeneous medium, the finite differences method is used. The soil is assumed to be a linear elastic continuum. Elasticity is a realistic assumption for soils when dealing with small strains and continuity is justified when the wavelengths of disturbances is significantly larger than the characteristic dimension of the medium (Santamarina et. al. 2001). In such a medium, the wave propagation is governed by wave parameters (frequency, wavelength, and amplitude) and material parameters (modulus of elasticity E, Poisson ratio ν, mass density ρ, and material attenuation α). No material damping is used in this study, because of its small effects at low-strain levels.

The material properties used in this study are ν=.0.2; ρ=1600 (kg/m^3), and C_p=114.9 (m/s). For simplicity, the stress dependent stiffness of soils is not considered. Furthermore, the small-strain stiffness is more sensitive to the state of stress in fine-grained soils (Feda 1982, Santamarina et al. 2001).

5 Model description

Figure 1 shows a general sketch of the two-dimensional model used in this study along with the applied load. A calibration procedure is utilized to assure that the model accurately estimates the important features of the R-waves propagating in a semi-infinite medium. The model inputs (overall sizes of the model, temporal and spatial increments, boundary conditions, maximum and minimum dynamic times, and source frequency content) are adjusted in a way that its outputs matches well with the theoretical observations (Lamb solution – Lamb 1904).

For the s- and v- models the uniform grid size is 750 (H) x 750 (V) and $\Delta t = 10^{-5}$s, whereas for T- and P- models a uniform grid of the size 1000(H) x 550(V) along with a $\Delta t = 3.8 \times 10^{-6}$s are chosen, for material type I. The stability criterion is considered for spatial and temporal descritizations (Itasca 2000). Quiet boundaries are used to reduce the amount of reflections from the boundaries (Lysmer and Kuhlemeyer 1969). In all the cases, the maximum dynamic time is restricted to t = 0.12 s and the boundaries are located as far from the void as practically possible, to mitigate the unwanted reflections.

Rectangular voids with different sizes are inserted in the s-model at 4.0 m from the source. Preliminary investigations on the s-model showed that after a distance of approximately two wavelengths from the source the error in phase velocities is less than 1%. The distance between the first receiver and the sourc is 3.16 m. According to Hiltuen and Woods (1989), the largest wavelength that can be extracted from a SASW test is equal to half of the offset value. Virieux (1986) suggested using at least 10 nodes per wavelength to control numerical dispersion, so the maximum reliable wavelength is assumed to be 10 times the grid size. The largest and smallest reliable wavelengths that can be extracted from the model are λ_{max}=1.58 m (f=41Hz) and λ_{min} =0.08m (f=801 Hz) respectively, for material type I.

To consider the effect of surface topography on the SASW results, two series of models with non-horizontal surfaces are studied. In model type T the whole surface is inclined, while in model type P, part of the surface is horizontal and part of it is sloped. The surface slopes vary from 1.75% to 3.5%. These are gentle slopes to avoid numerical errors due to grid geometry. In both models, voids with different sizes are included at 4 m distance from the source at different depths, and the responses on the surface are recorded and analyzed.

6 Dynamic source

A transient vertical displacement is used as the source, which generates surface waves of various frequencies. The frequency range of interest determines the type of the source function. The details of the source functions used in this study can be found in Nasseri-Moghaddam et. al. 2005.

7 Effect of lateral in-homogeneities on surface responses

The characteristics of the anomaly (i.e. size, embedment depth, shape of the anomaly, material properties, in-homogeneity, and mechanical impedance ratios) influence the surface response of a medium. Also the layered structure of the medium affects the surface response significantly. To reduce the complexity of the analysis, the effect of individual parameters is considered separately in this study. This paper focuses specially on the effect of the embedment depth of cavities on the surface response. Different types of noises, sources and inclined surfaces, are used to show the capabilities of the Attenuation Analysis of Rayleigh Waves method (AARW) for detecting a void and estimating its embedment depth (Nasseri-Moghaddam et. al. 2004).

8 Experimental methodology

In this study, voids are included in the s-model and the responses due to a transient loading are recorded on the surface. The size of the void is chosen to be 5%, 7%, 10%, 20%, 40% and 80% of the largest reliable wavelength available in the model. The embedment depths are also varied in the same range. Both of the x and y components of the surface displacements are recorded and the total surface displacement is calculated. To extend the applicability of the results presented here, normalized parameters are used. The normalized time

($\bar{t}$) and frequency ($\bar{f}$) are defined according to the following relationships (Gucunski et al. (1996)):

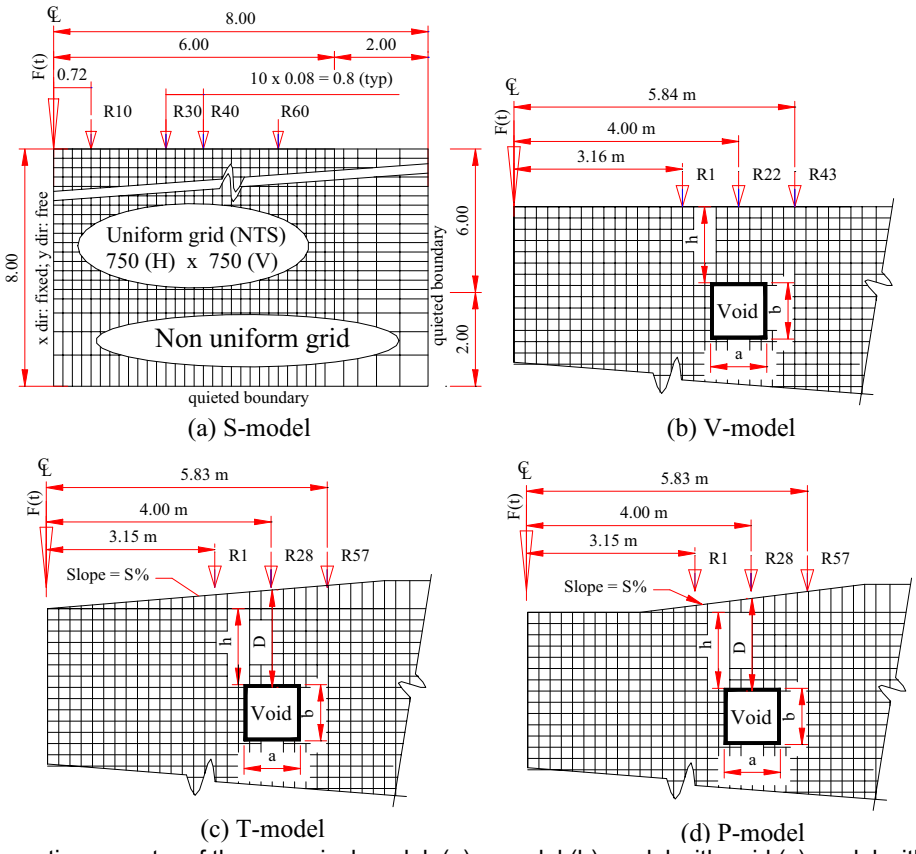

Figure 1: schematic geometry of the numerical model: (a) s-model (b) model with void (c) model with inclined surface type T (d) model with inclined surface type P

$$\bar{f} = \frac{f1}{C_R} \quad and \quad \bar{t} = \frac{tC_R}{1} \qquad (1)$$

where C_R, f and t are R-wave velocity, frequency, and time respectively. A unit-normalized time represents the time required by the R-wave to travel a unit distance, in this paper 1 meter. Normalized frequency equal to 1 represents the frequency for which the wavelength is equal to 1 m. All the distances and spatial dimensions are normalized to the largest reliable wavelength in the model (λ_{max}=1.58 m). The normalized scales are used in all graphs unless otherwise stated.

9 Time responses

A contour plot of the surface responses of a v-model is depicted in Figure 2. The normalized size and embedment depth of the void are 0.0709 and 0.0506 respectively (0.112 m and 0.080 m). Simulations with different void sizes and embedment depths reveal that when the R-wave encounters a lateral in-homogeneity part of its energy continues travelling with a slight phase shift after the anomaly. The rest of the energy is either reflected as R-wave or converted to body waves. Viktorov (1958) and deBremaecker (1963) reported a similar behaviour for a R-wave encountering a corner. The closer the void is to the surface, more frequencies are affected and thus the reflected/diffracted waves are stronger. Reduced interactions between the void and the incident wave take place, when the embedment depth is increased. This behaviour imposes a practical limitation on the largest embedment depth that can be detected with surface waves.

Results from the T- and P- models with different surface slopes, void sizes, and embedment depths also show the same trend. Though in the case of inclined surfaces, the embedment depth (D) of the void is different than the vertical distance between the void and the source (h). By increasing the slope – increasing the embedment depth- the interaction between the void and R-waves decreases.

Therefore the embedment depth at the top of the void is the dominant parameter that affects the surface response not the inclination of the surface when the surface slopes are small (slope < 3.5%).

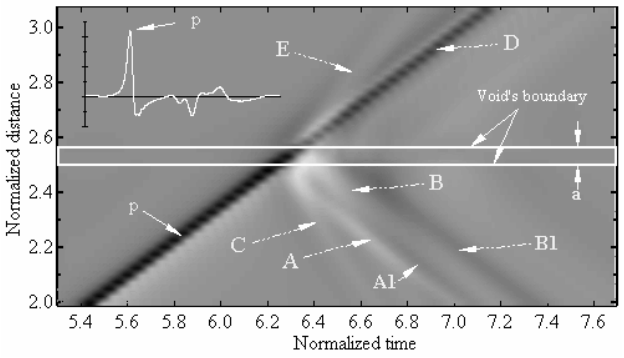

Figure 2: Contours of the time traces of the v-model, normalized to maximum response: a = 7%λ_{max} (0.112m) and h = 0.0506 (0.08 m)

10 Frequency Spectrums

A typical contour plot of frequency spectrums for the v-model is shown in Figure 3. Exactly before the void, a region with high-energy concentration is observed (region A). Other researchers (Gucunski 1996, Phillips 2001) also reported the same phenomenon. Experiments with different void sizes, embedment depths (same type of source), and surface slopes show that this energy concentration always occurs at the frequencies that carry most of the source energy. Further, they always occur between the void and the source. The amplification of the response in this region can exceed the response of the s-model by a factor of two. Also various experiments show that the peak values decrease by increasing the embedment depth of the void, and after a depth of about 0.2λ_{max} the amplification cannot be distinguished at all. For small slopes, the effect of surface inclination is negligible, and just the embedment depth of the void determines the amount of interaction that occurs.

Phillips et al. (2001) proposed a void detection method based on the location of the energy concentration in frequency spectrum. They verified the method by data obtained from a prototype and field measurements. Also Shokouhi and Gucunski (2003) reported a similar phenomenon, though they used wavelets to analyze the data. They also proposed a void detection method based on their numerical results. Although many of the details have been worked out, neither of these methods has been quantified and their applicability has not been determined. Moreover, experiments with anomalies filled with different materials show that the response amplification can be seen only when the acoustic impedance of the medium is approximately more than three times larger than the impedance of the anomaly.

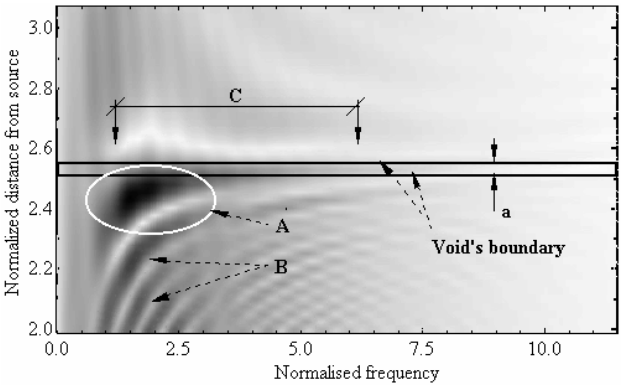

Figure 3: Frequency content of the model with void. a = 0.0506 (0.08 m) & h = 0.0506 (0.08 m)

The interaction of the incident wave with the void can be concluded from the strong ripples before the void (Figure 3), which are indications of reflected signals. Region C in the figure shows a zone with highly attenuated amplitudes. Physically, it can be concluded that the void acts as a damper and generates a shielded region after itself. Thus, a quantitative method to locate a void based on the amplification and attenuation of the response can be developed (Nasseri-Moghaddam et. al. 2004). In this method the Energy-Distance parameter at the location of any receiver z is defined as:

$$ED_z = \frac{E_z}{\max(E_z)} \quad where\ E_z = \sum_f \left| A_{f,z} \right|^2 \qquad (2)$$

where E_z is the signal energy at receiver z, the summation is calculated over the reliable frequency range, and $|A_{f,z}|$ is the amplitude of the spectrum at frequency *f* and receiver *z*. The energy-distance parameter (ED_z) is defined as the value of E_z normalized to the maximum value available in the vector. The maximum value of energy-distance parameter (ED_z) is equal to 1, and the smallest possible value is zero.

Figure 4 shows the values of energy-distance parameter calculated for both the x- and y-components of the surface displacement for different simulations. The vertical arrows in each graph show the location of the void boundaries. In all the cases, a local maximum can be distinguished right over the beginning of the void. Furthermore, a sharp decrease happens over the width of the void. As the embedment depth increases the slope of the curve over the void, decreases. Both of the x- and y- displacements show the same trend, though the peak in the ED parameter values for x-displacements are more conspicuous specially for the deeper voids. Moreover, in the case of inclined surfaces the NED values show similar behaviour.

11 Logarithmic decrement (L.D.)

The contour plot of the logarithmic decrements between the consecutive receivers for a v-model is demonstrated in Figure 5. Various experiments show that between the void and source low frequencies are magnified at farther distances from the void; whereas, higher frequencies are magnified closer to the void (curve A). The explanation for this behaviour is that larger wavelengths need larger distances to fully develop. So the effect of reflected waves with lower frequencies – larger wavelengths – can be seen at farther distances. Consequently, the maximum magnification or attenuation curves are bended before the void (curves A and B). After the void the pattern of maximum attenuation curve is almost parallel to the void boundary (curve C). The reason is that after the void, its effect on the already developed waves is observed- all of developed wavelengths are influenced at almost the same location. Moreover in front of the void the waves are first magnified and then attenuated; whereas, after the void they are attenuated first and then magnified. This trend of the L.D. pattern is used in AARW method to locate the void.

Simulations with different embedment depths reveal that the wavelength of the largest frequency at which a local peak in attenuation occurs (curve C) corresponds to the embedment depth of the void. The physical interpretation of this observation is that the void is excited by the frequencies whose wavelengths are close to or larger than its embedment depth. Consequently, the wavelengths that are smaller than the embedment depth propagate almost without any change. The consistency between the embedment depth of the void and the wavelength of the cut off frequency is used to determine the embedment depth of the void quantitatively. In AARW method, the normalized amplified logarithmic decrement (NALD) is calculated for each frequency as in equation 3 .(Nasseri-Moghaddam et. al. 2004).
.

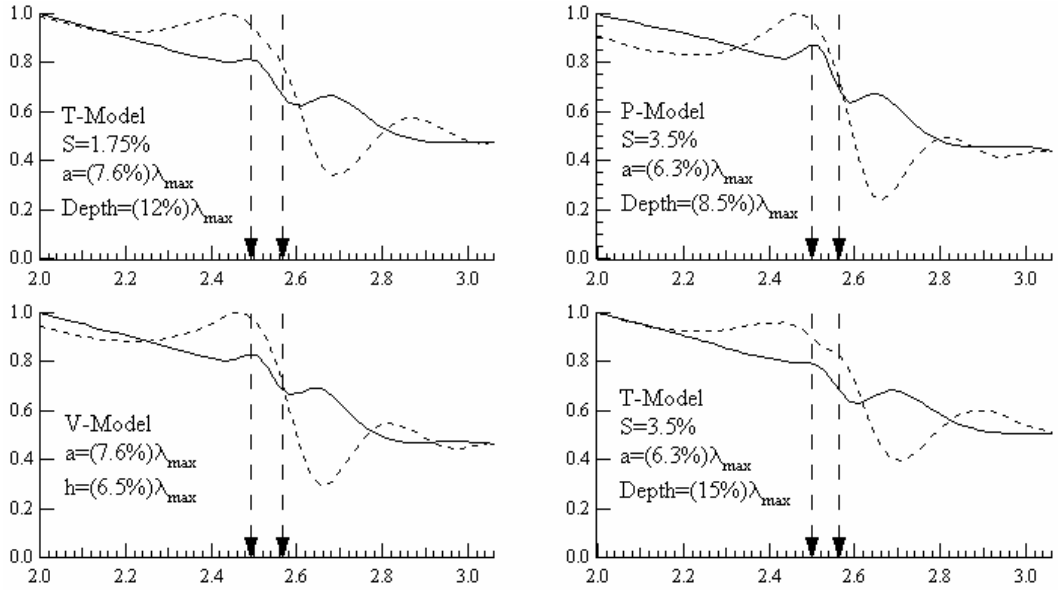

Figure 4: Variation of Normalized Energy-Distance parameter (NED parameter) with normalized distance from the source (Horizontal axis). Dashed graphs correspond to x displacement components (λ_{max} = 1.58 m)

$$NALD_j = \frac{ALD_j}{\max(ALD)} \quad where$$

$$ALD_j = \sum_{z=1}^{z_{max}-1} \left\{ Ln\left(\frac{U_{j,z} + \alpha}{U_{j,z+1} + \alpha} \right) \right\}^{\beta} \qquad (3)$$

where ALD_j is the value of amplified logarithmic decrement at frequency f_j, z_{max} is the maximum number of receivers, $U_{j,z}$ and $U_{j,z+1}$ are the spectral amplitudes at frequency f_j and receivers z and $z+1$ respectively. α is an experimental constant value to reduce the effect of noise. The logarithmic decrement is very susceptible to the ratio of the spectral amplitudes at consecutive receivers. Hence, there is a potential to obtain large values even for very small frequency magnitudes (noise). By introducing α in equation 3, the effect of magnitudes smaller than α will be filtered out. β is an arbitrary constant to magnify the

peaks. Experiments with different values showed that, for the cases investigated in this study, the values of α and β – as defined in equation 3– give reasonable results. Figure 6 depicts the NALD values calculated from the y- components of surface displacements for different cases. In each graph the arrow shows the frequency, for which the wavelength is equal to the embedment depth of the void. For all of the cases, a peak occurs at the cut off frequency. In all of the cases the peak is the last local maximum that can be measured. Experiments with different source types confirmed the mentioned result. The error of the estimation is smaller for shallow voids. After an embedment depth of about (20%)λ_{max}, the error in the estimation of h is be more than 50%.

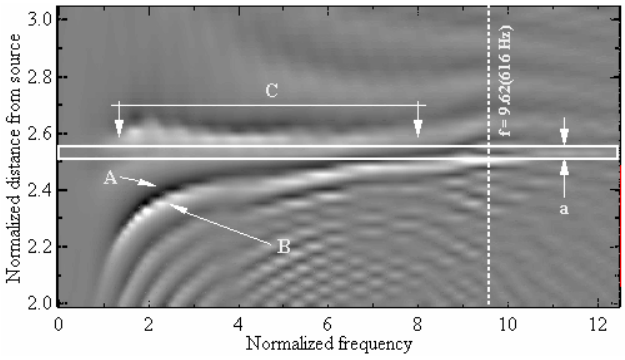

Figure 5: Logarithmic decrement of the model with void: case a – a = 0.05 and h = 0.066

12 Conclusions

This paper verifies the validity of the AARW method, which was proposed by the authors for the detection of a void and estimation of its embedment depth, in different cases. To take into account the effect of noise, source type and surface topography, different numerical models are constructed. The conclusions of the study are as follows:

- Due to the interaction of void with incident wave, part of the energy is reflected, part is transferred and part is converted into body waves.
- Due to the scattering effect of the anomaly the transferred wave is attenuated.
- The attenuation analysis of surface waves (AASW) technique, showed to be a promising tool for detecting a void and estimating its embedment depth.

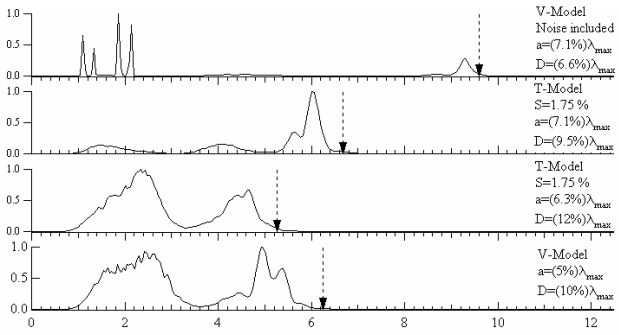

Figure 6: Normalized amplified logarithmic decrement values – NALD values. Horizontal axis shows the frequency normalized to C_R=64.08 m/s.

The presented analysis did not consider the practical restrictions available in the field, such as: existence of other sources of vibration, inherent in-homogeneities of a soil system, and limiting characteristics of the equipment. Hence a crucial improvement of the method is its application to the real field data. It is recommended to collect and analyze both x- and y- surface displacements while performing the MASW test. Also running the test from both sides of a receiver arrangement improve the accuracy of the results. The investigation of the combined effects of lateral and vertical in-homogeneities on the propagation of Rayleigh waves, and the use of the AASW method in more general cases are the subjects of ongoing research.

13 References

Al-Hunaidi, M.O., 1993, "Insights on the SASW nondestructive testing method. Can. J. Civ.Eng., V.20,pp. 940-950

deBremaecker, J. Cl., 1963, "Transmission and reflection of Rayleigh waves at corners. Geophysics, Vol. 23, pp. 253 – 266

Feda, j., 1982, "Mechanics of particulate materials: the principles. Elsevier Scientific Publishing Company, New York, 447 pp.

Ganji, V., Gucunski, N., Nazarian, S., 1998, "Automated Inversion Procedure for Spectral Analysis of Surface Waves. Journal of Geotechnical and Geoenvironmental Engineering , ASCE, V. 124, No. 18

Graff, K.F., 1991, "Wave motion in elastic solids. Mineola, NY. Dover publications

Gucunski, N., Ganji, V. & Maher M.H.,1996, "Effects of obstacles on Rayleigh wave dispersion obtained from the SASW test. Soil Dynamics and Earthquake engineering, vol. 15, pp 223-231

Gucunski, N., Woods, R.D., 1992, "Numerical Simulation of the SASW test. Soil Dynamics and Earthquake Engineering 11, pp. 213 – 227

Hall, J.R., Richart, F.E., 1964, "Dissipation of elastic wave energy in granular soils. Journal of the soil mechanics and foundations division, ASCE, November 1963, SM6, pp. 27 – 56

Hardin, B.O., Drnevich, V.P., 1972, “Shear modulus and damping in soils: design equations and curves. Journal of the soil mechanics and foundations division, ASCE, July 1972, SM7, pp. 667 – 692

Hiltunen, D.R., Woods, D., 1989, “Influence of Source and Receiver Geometry on the Testing of Pavements by the Surface Waves Method. Nondestructive testing of pavements and back calculation of muduli, ASTM ATP 1026, pp. 138-154

Itasca consulting group, 2000, “FLAC: Fast Lagrangian Analysis of Continua Users Guide. Itasca consulting group, Inc., Minneapolis, Minnesota

Jones, R., 1962, “Surface wave technique for measuring the elastic properties and thickness of roads: theoretical development. British journal of applied physics, Vol. 13, pp. 21 – 29

Lamb, H., 1904, “On the propagation of Tremors over the surface of an elastic Solid. Philosophical Transactions of the Royal society of London, Series A 203, pp. 1 – 42

Lysmer, J., and Kuhlemeyer, R., August 1969, “Finite Dynamic Model For Infinite Media. Journal of Engineering Mechanics Division, pp. 859 – 877

Miller, G.F., Pursey, H., 1954.”The field and radiation impedance of mechanical radiators on the free surface of a semi-infinite isotropic solid. Proceedings of the Royal sociaety of London, series A, Vol 223, pp. 521-541

Nasseri-Moghaddam, A., Cascante, G., Phillips, C., and Hutchinson, J. 2004. “A new quantitative procedure to determine the location and embedment depth of a void with surface waves. Proc. of the Symposium on the Application of Geophysics to Engineering and Environmental Problems, Colorado Springs, Colorado

Nasseri-Moghaddam, A., Cascante, G., Phillips, C., and Hutchinson, J. 2005. “A new quantitative procedure to determine the location and embedment depth of a void with surface waves. Journal of Environmental and Engineering Geophysics (Submitted for publication)

Nazarian, S., Stokoe, K. H. 1984, “In situ shear wave velocities from spectral analysis of surface waves. Proc. Of the eigth world conf. On earthquake engineering, Sanfrancisco, California, Vol III, July 21 - 28, pp. 31 – 38

Phillips, C., Cascante, G., and Hutchinson, J., 2001, “Numerical simulation of seismic surface waves. 54th Canadian Geothecnical Conference, Calgary, Alberta, September 2001, pp. 1538 – 1545

Reynolds, J.M., 1997, ‘An introduction to applied and environmental geophysics. England: John Wiley and sons

Santamarina, J.C., Klein, K.A., Fam, M.A., 2001, “Soils and waves. John Wiley and Sons Inc., New York

Sheu, J.C., Stokoe II, K.H., and Rosset, J.M., 1988, “Effect of reflected waves in SASW testing of pavements. Transp. Res. 1196, Transportation research board, National research council, Washington, D.C., pp. 51 – 61

Shokouhi, P., Gucunski, N., 2003, “Application of Wavelet transform in detection of shallow cavities by surface waves. SAGEEP 2003

Stokoe, K.H. II, Nazarian, S., 1985, “Use of Rayleigh waves in liquifaction studies, Measurement and use of shear wave velocity for evaluating dynamic soil properties. Proceedings of a geotechnical engineering division session at ASCE convention, Denver, Colorado, May 1, pp. 1 – 17

Viktorov, I.A., 1958, “The effects of surface defects on the propagation of Rayleigh waves. Soviet Physics, Doklady, 3, pp. 304 – 306

Virieux, J., 1986, “P - SV wave propagation in heterogeneous media: Velocity- Stress finite difference method. Geophysics, V. 51